

Overcoming drug resistance with on-demand charged thermoresponsive dendritic nanogels

Aim: To develop nanogels (NG) able to modulate the encapsulation and release of drugs, in order to circumvent drug resistance mechanisms in cancer cells. **Materials & methods:** Poly-*N*-isopropylacrylamide–dendritic polyglycerol NG were semi-interpenetrated with 2-acrylamido-2-methylpropane sulfonic acid or (2-dimethylamino) ethyl methacrylate. Physico-chemical properties of the NGs as well as doxorubicin (DOXO) loading and release were characterized. Drug delivery performance was investigated *in vitro* and *in vivo* in a multidrug-resistant tumor model. **Results:** Both the DOXO loaded semi-interpenetrating polymer network NGs were more efficient in multidrug resistant cancer cell proliferation inhibition studies. *In vivo*, the DOXO loaded NG semi-interpenetrated with 2-acrylamido-2-methylpropane sulfonic acid was able to overcome drug resistance and reduce the tumor volume to about 25%. **Conclusion:** The innovative semi-interpenetrating polymer network NGs appear to be promising drug carriers for drug resistant cancer therapy.

First draft submitted: 15 August 2016; Accepted for publication: 25 October 2016; Published online: 23 November 2016

Keywords: doxorubicin carrier • drug resistance • semi-interpenetrated PNIPAM

Although great advances have been made in the field of cancer therapy, cancer is still one of the main causes of death worldwide [1]. Nanotechnology has attracted a lot of attention as a solution to overcome this problem [2]. Among others, smart materials that are able to release drugs on demand are being explored for chemotherapeutic treatment of cancer [3]. Doxorubicin (DOXO) is one of the most widely used chemotherapy agents including three forms of nanomedicine on the market or in clinical trials, DOXIL[®], Myocet[®] and ThermoDox[®] [4]. The major drawback of chemotherapy is that cancer cells can develop drug resistance [5], which is typically mediated by P-glycoprotein, an efflux pump which decreases the intracellular drug concentration [6]. In fact, drug resistance occurs in over 50% of patients in the clinic [7]. Different nanocarriers have proved to be effective for delivering DOXO to the resistant

cell lines. The mechanism of action of these nanocarriers is mostly based on the release of the drug inside the cell, thus avoiding P-glycoprotein-mediated drug resistance [8]. As shown in previous studies [9–12], in a system for overcoming drug resistance, it is important that the drug is strongly encapsulated and not released before cellular uptake and transport to the cytoplasm. Among the different carriers, nanogels (NGs) are the most interesting systems due to their hydrophilicity and high encapsulation efficiencies [13,14]. NGs are crosslinked polymer networks that are able to absorb large quantities of water. Smart NGs respond to an external stimulus, such as pH, light or temperature [15–17]. In particular, thermoresponsive NGs are mostly used as drug delivery systems because they can be easily triggered.

Poly-*N*-isopropylacrylamide-based (PNIPAM) NGs are widely used as thermore-

Maria Molina¹, Stefanie Wedepohl¹, Enrico Miceli^{1,2} & Marcelo Calderón^{*1,2}

¹Institute for Chemistry & Biochemistry, Freie Universität Berlin, Takustr. 3, 14195 Berlin, Germany

²Helmholtz Virtual Institute “Multifunctional Biomaterials for Medicine”, Kantstr. 55, 14513 Teltow, Germany

*Author for correspondence:
Tel.: +49 30 83859368

marcelo.calderon@fu-berlin.de

sponsive drug delivery systems, because PNIPAM exhibits a lower critical solution temperature (LCST) of approximately 32°C, which is close to body temperature [18]. Therefore, the polymer can undergo temperature-induced reversible coil-to-globule phase transitions, which can influence the release behaviors of encapsulated drugs [19].

Our group has developed thermoresponsive dendritic NGs composed of a combination of thermoresponsive polymers with dendritic polyglycerol (dPG), that provide sizes in the biomedically relevant range between 50 and 200 nm [20–26]. The presence of dPG as a macro-crosslinker, attached via a biodegradable ester linkage, provides high biocompatibility and hydrophilicity and, more importantly, can prevent the precipitation of the NGs in the collapsed state above the transition temperature (T_p). In order to modify the properties of PNIPAM NGs, different co-polymers [27,28] and composites [29–31] have been prepared and changes, e.g., in the release rate, the swelling behavior and lower critical solution temperature were obtained.

Novel materials where a polymer has been interlaced with another network are called either interpenetrating polymer networks (IPN) or semi-interpenetrating polymer networks (SIPN) [32]. The incorporation of a second polymer allows to improve the mechanical properties of the material and to introduce new functionalities without significantly affecting the thermal sensitivity of the gel [33].

Considering the state-of-art and with the intention of developing a drug delivery system with a slow release rate for overcoming drug resistance in cancer, we describe herein the synthesis of ‘on demand charged’ thermoresponsive dendritic NGs by semi-interpenetrating pH sensitive polymers into PNIPAM/dPG NGs (Figure 1). (2-dimethylamino)ethyl methacrylate (DMAEM) and 2-acrylamido-2-methylpropane sulfonic acid (AMPS) were chosen as the pH sensitive monomers. We characterized the physico-chemical properties of the novel materials as well as their DOXO loading capacities and release profiles. The cytotoxicity and cellular uptake of the bare SIPN NGs was studied before the performance as drug carriers in a biological context was evaluated using a DOXO resistant cell line *in vitro* and a resistant tumor model *in vivo*. Taken together, the results of the present study support the use of SIPN NGs as a new strategy to circumvent drug resistance mechanisms in cancer cells.

Materials & methods

The following chemicals were used as purchased: N-isopropylacrylamide (NIPAM; Sigma-Aldrich), AMPS (Sigma-Aldrich), DMAEM (Sigma-Aldrich),

acryloyl chloride (AC; 96% Fluka), extra dry dimethylformamide (DMF; 99.8% Acros), triethylamine (TEA; Acros), ammonium persulphate (APS; 98% Sigma-Aldrich), sodium dodecyl sulphate (SDS; 98% Acros), N,N,N',N'-tetramethylethylenediamine (TEMED; 99% Sigma-Aldrich).

Synthesis of acrylated dendritic polyglycerol (dPG-Ac 10%)

dPG with average Mw of 10 kDa was synthesized according to previously reported methodologies [34]. The dPG was dried overnight under vacuum at 140°C. A solution of AC (0.65 mmol, 52 μ l) in dry DMF (1 ml) was added dropwise to a stirred solution of dPG (1 g, 10 kDa, 13.51 mmol OH equivalent) and TEA (1.08 mmol, 150 μ l) in DMF (7 ml) at 0°C. The reaction was left at r.t. for at least 4 h. A small amount of water was added into the reaction mixture in order to dissolve the precipitated salt. The reaction mixture was purified by dialysis membrane (molecular weight cut-off [MWCO] 2 kDa) in water for at least 24 h. The acrylated dPG was preferably used directly after purification. Otherwise the product was stored in dark, at 4°C in the presence of p-methoxyphenol and dialyzed again before usage. $^1\text{H-NMR}$ (500 MHz, D_2O), δ : 3.2–4.3 (m, 5 H, polyglycerol scaffold protons), 5.88–6.00 (m, 1 H, vinyl), 6.08–6.28 (m, 1 H, vinyl), 6.32–6.44 (m, 1 H, vinyl).

Synthesis of NGs

PNIPAM- dPG NGs were synthesized following the procedure described before by our group [24]. Briefly, 100 mg of monomers, 67 wt% NIPAM and 33 wt% of dPG-Ac, SDS (1.8 mg) and APS (2.8 mg) were dissolved in 5 ml of distilled water. Argon was bubbled into the reaction mixture for 15 min. The mixture was stirred under argon atmosphere for another 15 min, transferred into a hot bath at 68°C and polymerization was activated after 5 min with the addition of catalytic amount of TEMED (120 μ l). The mixture was stirred at 500 rpm for at least 4 h. The product was purified by dialysis membrane (MWCO 50 kDa) in water for 2 days and then lyophilized to obtain a white solid. $^1\text{H-NMR}$ of PNIPAM-33% dPG NGs: (500 MHz, D_2O), δ : 1.13 (s, 6 H, isopropyl groups of NIPAM), 1.57 (2 H, polymer backbone), 2.00 (1 H, polymer backbone), 3.35–4.10 (6 H, polyglycerol scaffold protons + 1 H NIPAM).

Alternatively, fluorescein isothiocyanate (FITC)-labeled NGs were synthesized to be used in cellular uptake studies. For this purpose, dPG was labeled with FITC before acrylation. Briefly, FITC (4.7 mg) was dissolved in a small amount of DMSO (i.e., 100 μ l and 60 mg of dPG-NH2 (~13.5 amino groups (10%)) and

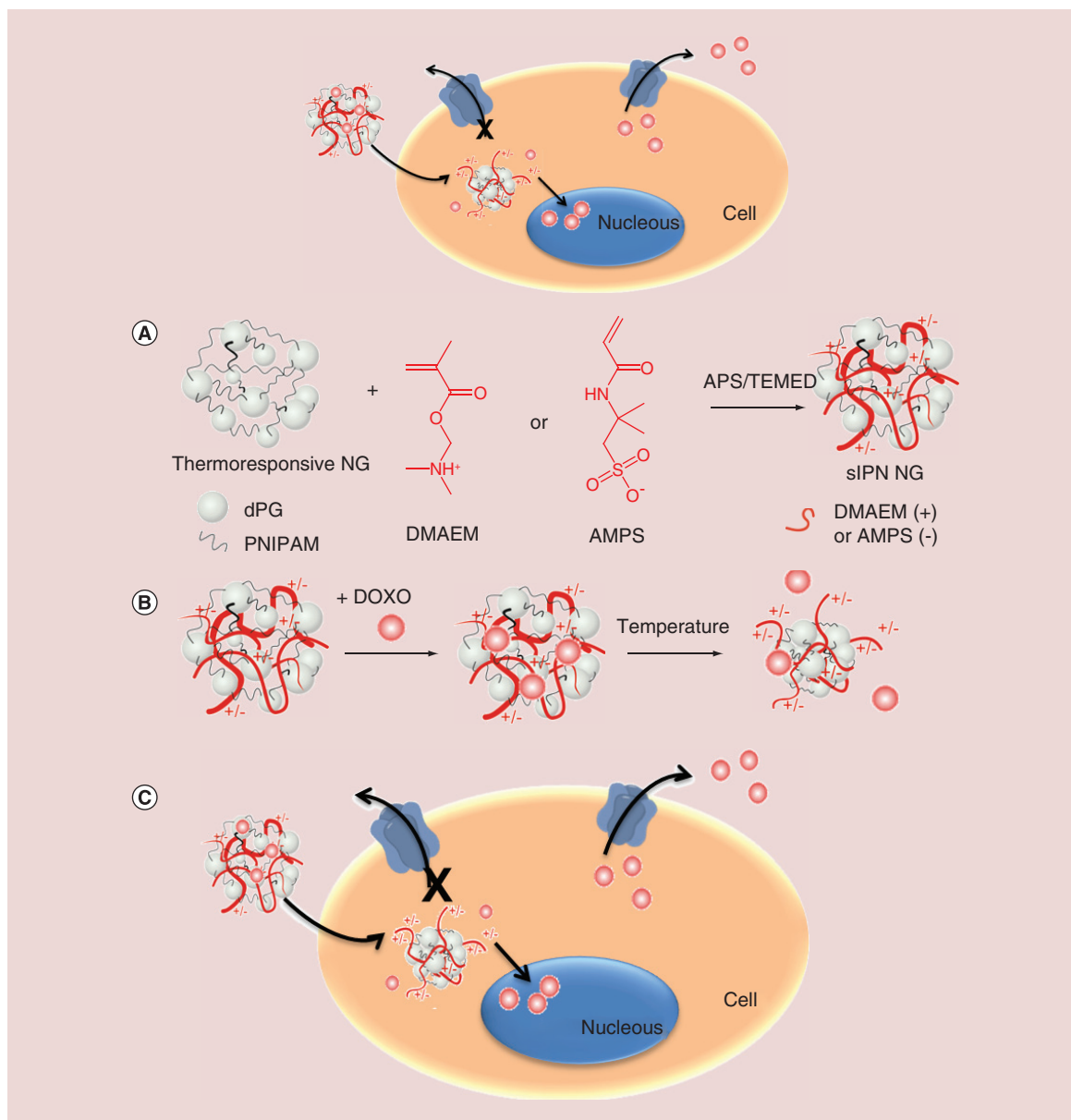


Figure 1. Schematic representation of (A) SIPN NG from PNIPAM/dPG NG and charged monomers, (B) encapsulation and release of DOXO and (C) proposed mechanism to overcome multidrug resistance by slow drug release in the near of the cell nucleus.

DOXO: Doxorubicin; PNIPAM: Poly-*N*-isopropylacrylamide.

2 ml of phosphate-buffered saline (PBS; 10 mM, pH = 7.4) were added. The reaction took place at r.t. for 1 h. Successful coupling of FITC was checked by thin layer chromatography (TLC). The product was purified by size-exclusion chromatography (SEC) with Sephadex G25 fine and then lyophilized.

Synthesis of SIPN NGs

For the synthesis of the SIPN, 40 mg of dry PNIPAM/dPG NG were swollen in a solution of the monomer to be interpenetrated (5, 10 or 20 mol% AMPS or

DMAEM referred to NIPAM mol) and APS for 2 h. The reaction mixture was bubbled with argon for 10 min and transferred to an ice bath. After 5 min, the *in situ* polymerization was activated by the addition of TEMED (100 μ l). The reaction was carried out for 2 or 12 h. The products were purified by dialysis (MWCO 50 kDa) in water for 2 days and then lyophilized to obtain a white solid. The effective semi-interpenetration was tested by Fourier transform infrared spectroscopy (FT-IR) using a Bruker IFS 66 FT-IR spectrophotometer in the range of 4000–500 cm^{-1} .

Alternatively, FITC-labeled SIPN NGs were synthesized using FITC-labeled PNIPAM/dPG as starting material.

Characterization

The size and phase transition (T_p) of the nanoparticles were studied by dynamic light scattering (DLS) using a Nano-ZS 90 Malvern equipped with a He-Ne laser ($\lambda = 633$ nm) under scattering of 173° . All the samples were maintained at the desired temperature for 5 min before testing, which was found to be suitable to achieve stabilization. The samples were prepared by dissolving 1 mg of dry NG in 1 ml of HEPES buffer solution pH 6, 1 day prior to the experiments. Particle size and size distribution are given as the average of three measurements from the volume distribution curves. T_p was also determined by the cloud point temperature method measured on a Cary 100 Bio UV-Vis spectrophotometer equipped with a temperature-controlled, six-position sample holder. HEPES buffered NGs solutions (1 mg ml^{-1}) at pH 6 were heated at $0.2^\circ\text{C min}^{-1}$ while monitoring both the transmittance at 500 nm (1 cm path length) and the solution temperature (from 25 to 65°C), as determined by the internal temperature probe. The T_p of each NG was determined using the minimum of the first derivative of transmittance versus temperature. The shape of the NGs was studied by transmission electron microscopy (TEM). TEM was performed on Hitachi SU 8030 scanning electron microscope operating at 30 kV. For preparation, a droplet (2 μl) of the sample solution was attached onto a carbon-coated copper grid and dried by air followed by a droplet of uranyl acetate (1%). The zeta (ζ) potential of the NGs was determined below and above the T_p with a NanoZetaSizer.

Post-synthetic encapsulation of DOXO

DOXO was encapsulated in the previously synthesized NGs. DOXO (0.75 mg) in HEPES solution was added to the dry NGs (1.5 mg) in a microcentrifuge tube. The NGs were allowed to swell for 24 h. The samples were centrifuged in a filter unit of 3000 Da three times for 10 min at 5000 rpm, and the concentration of DOXO in the filtrate was determined via UV-Vis spectroscopy ($\epsilon = 8800 \text{ M}^{-1}\text{cm}^{-1}$).

The loading capacity and loading efficiency of the drug in the NGs were calculated using Equations 1 & 2:

- Loading capacity = $(w_i - w_f) / w_{ng} \times 100\%$
- Loading efficiency = $(w_i - w_f) / w_i \times 100\%$

where w_i , w_f and w_{ng} are the amounts of drug initial, final and the weight of NGs, respectively.

Release study

The release of the drugs was studied by a dialysis method. The centrifuged NGs with the encapsulated drug were re-dissolved in buffer at pH 5 or 7.4. Briefly, 0.5 ml of the DOXO-loaded NG solution (1.5 mg) was placed in a 50 kDa MWCO dialysis tube and dialyzed against 10 ml of buffer with gentle stirring. Different pH (5, 6.8 and 7.4) and temperatures (r.t, 37 and 40°C) conditions were tested in order to study the influence of these stimuli to the release. At certain time intervals, 200 μl of the outer solution were taken for UV-Vis analysis and replaced by addition of fresh release media. The results were plotted as the cumulative release (%) versus time.

Biological studies

HeLa cells (German Collection of Micro-organisms and Cell Cultures [DSMZ] #ACC57) were routinely maintained in RPMI medium with 2 mM L-glutamine, 10% FCS, 1% penicillin/streptomycin and 1% nonessential amino acids (Life Technologies) at 37°C and 5% CO_2 . KB-V1 cells (DSMZ # ACC 149) were maintained in Dulbecco's modified Eagle medium with 15% FCS and 1 μM DOXO at 37°C and 5% CO_2 .

Cytotoxicity assay

1×10^5 cells ml^{-1} were seeded into 96-well plates and incubated overnight at 37°C and 5% CO_2 . The next day, medium was replaced for 50 μl fresh medium and 50 μl dilutions of the test compounds (in triplicates). After 48 h of incubation at 37°C or 40°C , medium with compounds was discarded and 10 μl MTT (5 mg ml^{-1} stock solution in PBS) was added in 100 μl fresh medium. After incubation for 4 h at 37°C and 5% CO_2 , the supernatant was discarded and 100 μl isopropanol with 0.04 M HCl was added. Absorbance was read in a Tecan Infinite Pro M200 microplate reader at 570 nm. Assays were repeated three-times independently. Relative cell viabilities were calculated by dividing the average absorbance values by the absorbance value of untreated cells.

Cellular uptake studies

1×10^5 HeLa cells ml^{-1} were seeded on cover slips in 24-well plates and grown overnight. A total of 200 μg of FITC-labeled NG in fresh growth medium were then incubated with the cells for 7 h at 37°C and 5% CO_2 . Afterward, the medium and NGs were removed and the cells were washed three-times with 1 ml PBS and then fixed in 10% neutral buffered formalin for 20 min. After three-times washing with PBS, nuclei and cytoskeleton were stained with 2.5 $\mu\text{g ml}^{-1}$ DAPI and 1:500 diluted PromoFluor-590 phalloidin (Promo-

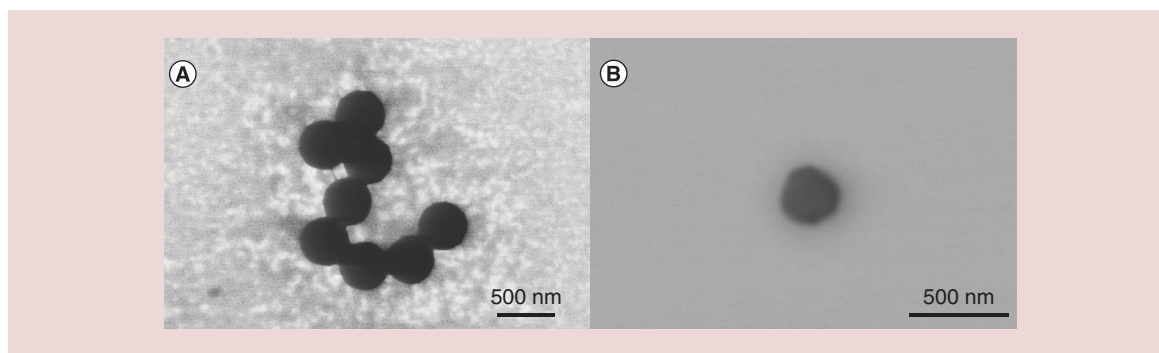


Figure 2. TEM images of (A) PNIPAM-s-AMPS and (B) PNIPAM-s-DMAEM.

AMPS: 2-acrylamido-2-methylpropane sulfonic acid; DMAEM: (2-dimethylamino) ethyl methacrylate; PNIPAM: Poly-*N*-isopropylacrylamide.

Kine) in PBS for 30 min. Cover slips were washed with PBS again, rinsed in water and mounted on microscope slides using ProTaq MountFluor mounting medium (Quartett, Germany). After drying overnight, samples were scanned with a Leica SP8 confocal laser scanning microscope and images were acquired with LASAF software.

In vivo studies

In vivo studies were performed in accordance with all national or local guidelines and regulations as described in the approved Tierversuchsantrag A 0452/08 (Landesamt Berlin für Gesundheit) from 28.11.2012 for the EPO GmbH Berlin-Buch.

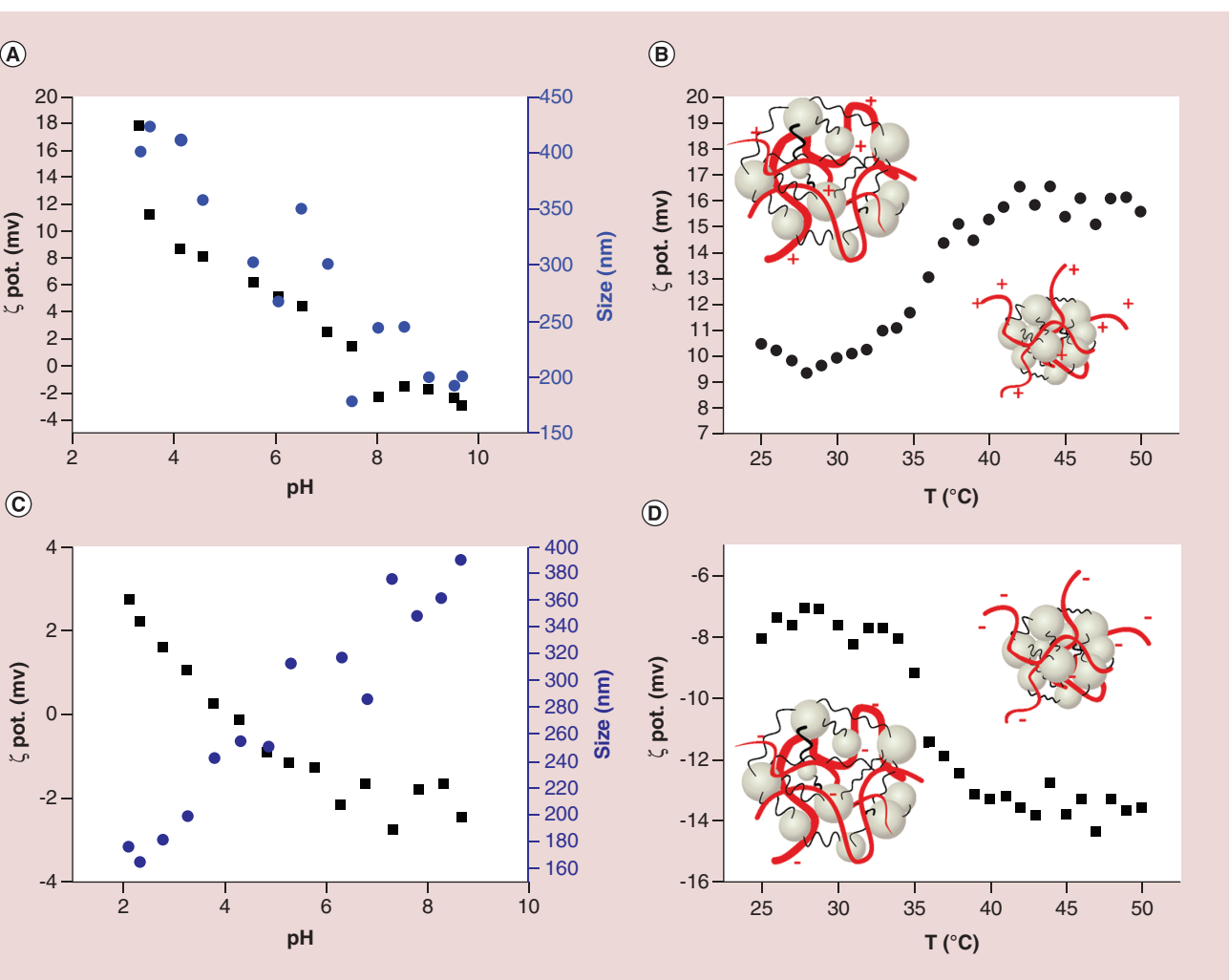
The tolerability and therapeutic effect of DOXO-loaded NGs was studied on adriablastin resistant MaTu carcinoma in nude mice. This cell line has been originally described as derived from a human mammary tumor, but has been found to be a mutated HeLa deriv-

ative [35]. 1×10^7 MaTu/ADR cells were transplanted subcutaneously into each female nude mouse (Charles River) at day 0. Mice were stratified on day 6, when the mean tumor volume (TV) was $0.105 \pm 0.021 \text{ cm}^3$, into eight groups with eight mice each. The mean TV at this time was $0.107\text{--}0.110 \text{ cm}^3$ per group. The mice were intravenously injected with PNIPAM/dPG, PNIPAM-s-AMPS, PNIPAM-s-DMAEM mixed or, in parallel, loaded with DOXO, or free DOXO as control at a concentration of 8 mg kg^{-1} . The treatment was done on day 6 and 13, followed by monitoring until day 39. Two to three-times a week, body weight and TV were measured; additionally, the blood composition was tested. For this, blood samples were drawn from the retro-orbital sinus under iso-flurane anesthesia 3 days after the first treatment and at the end of the experiment (day 9 and 39, respectively). Platelet and lymphocytes numbers were determined using a ZellDyn Emerald device. The experiment was finished on day 39.

Table 1. Properties of the synthesized nanogels.

NG	Polymerization time second polymer [h]	ζ -potential at 25°C [mV] ^{a)}	Tp [°C] ^{b)}
PNIPAM/dPG	–	-2.1	36.0
PNIPAM-s- 2% AMPS [†]	2	-2.7	35.5
PNIPAM-s- 2% AMPS [‡]	12	-3.9	37.0
PNIPAM-s- 10% AMPS	12	-6.7	36.5
PNIPAM-s- 20% AMPS	12	-12.2	37.0
PNIPAM-s- 2% DMAEM [†]	2	-0.8	36.5
PNIPAM-s-2% DMAEM [‡]	12	2.2	37.0
PNIPAM-s- 10% DMAEM	12	3.0	36.5
PNIPAM-s- 20% DMAEM	12	10.4	36.5

[†]Determined by Zetasizer in HEPES buffer at pH 6.
[‡]Determined by UV-Vis in HEPES buffer at pH 6.
 AMPS: 2-acrylamido-2-methylpropane sulfonic acid; DMAEM: (2-dimethylamino) ethyl methacrylate.



3. Influence of the pH (left) and temperature (right) in size and ζ potential of (A & B) PNIPAM-s-DMAEM and (C & D) PNIPAM-s-AMPS.
 S. 2-acrylamido-2-methylpropane sulfonic acid; PNIPAM: Poly-*N*-isopropylacrylamide.

Results

Synthesis & characterization of SIPN NGs

NGs with positive (PNIPAM-s-DMAEM) or negative (PNIPAM-s-AMPS) charges were synthesized by semi-interpenetration and *in situ* polymerization of the corresponding pH sensitive monomer into PNIPAM/dPG NGs (Figure 1). With this method, spherical NGs of ~300 nm at pH 7 were obtained, as it can be observed by TEM (Figure 2). Furthermore low polydispersity index of ~0.1 were measured by Dynamic Light Scattering (data not shown).

The charge density could be controlled by the ratio of pH sensitive monomer to NG as well as by polymerization time. The successful semi-interpenetration was proven by FT-IR (Supplementary Figure 1, ESI). In the case of PNIPAM-s-AMPS NGs, a new band appeared at 1050 cm^{-1} corresponding to the S=O stretching. When DMAEM was semi-interpenetrated within the

NGs, an enhancement in the amide band could be observed at 1721 cm^{-1} , while all the PNIPAM and dPG bands were still present.

After semi-interpenetration of the PNIPAM/dPG NGs, the absolute ζ -potential value of the network increased, which is shown in Table 1 along with the properties of the synthesized NGs. When the NG was semi-interpenetrated with the cationic or anionic polymer, the ζ -potential was more positive or negative, respectively. The ζ -potential also increased with higher percentages of the pH sensitive polymer in the network or with the polymerization time. The T_p's of the NGs did not change after semi-interpenetration with the pH sensitive polymers.

Two different behaviors could be obtained depending on the chosen polymer for the semi-interpenetration. As a general tendency, the size of the NG increased with the charge of the network. Thus, upon

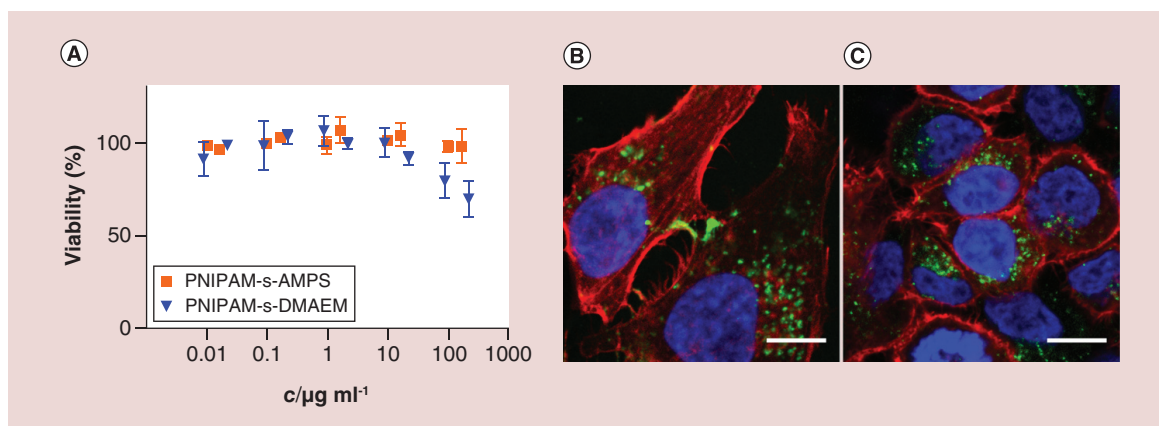


Figure 4. Biological evaluation of sIPN NGs (A) Cytotoxicity profile after 48 h of exposition at 37°C as determined by MTT test. (B & C) Cellular uptake of FITC-labeled NGs into HeLa cells (B) PNIPAM-s-DMAEM, (C) PNIPAM-s-AMPS. Blue areas represent the DAPI stained nucleus and red areas represent the phalloidin stained cytoskeleton of the cells. Shown is the merged image. Scale bar: 10 μm . AMPS: 2-acrylamido-2-methylpropane sulfonic acid; DMAEM: (2-dimethylamino) ethyl methacrylate; PNIPAM: Poly-*N*-isopropylacrylamide.

increase of the pH, the PNIPAM-s-DMAEM NGs decreased in size and the PNIPAM-s-AMPS NGs increased (Figure 3A & C). The opposite trend in size is due to the apparition of the charges, while the trend in ζ potential is the same the net charge is not. In the case of PNIPAM-s-DMAEM NGs, the size decreased at higher pH (pKa 6.8) from ~ 430 nm at pH 3 to ~ 175 nm at pH 10 with a change in the ζ -potential from 20 to -2 mV. The ζ -potential of PNIPAM-s-AMPS NGs (pKa -2) changed from 3 to -3 mV with the increase of pH from 2 to 10, followed by an increase of size from 150 to 400 nm.

After analyzing the properties of the different NGs we decided to continue the study using the 10% sIPN NGs in order to have charges enough to ensure a good encapsulation, but not too many that would inhibit the release of the drug.

Cytotoxicity & cellular uptake of sIPN NGs

In order to analyze the feasibility of the prepared materials for biomedical applications, first the *in vitro* cytotoxicity of the bare SIPN NGs (PNIPAM-dPG/AMPS 10% and PNIPAM-dPG/DMAEM 10%) was studied in HeLa cells by MTT assay (Figure 4A). Both carriers

did not reduce relative cell viability below 70% up to a concentration of ~ 200 $\mu\text{g ml}^{-1}$. To study the *in vitro* cellular uptake of the bare NGs, FITC-labeled NGs were exposed to HeLa cells for 7 h and after fixing and staining, were visualized by confocal laser scanning microscopy (Figure 4B & C). Cellular uptake could be clearly detected for PNIPAM-s-AMPS and PNIPAM-s-DMAEM NGs as a punctate pattern in the perinuclear region within the cells, indicating cellular compartments of the endocytotic pathway.

DOXO encapsulation & release

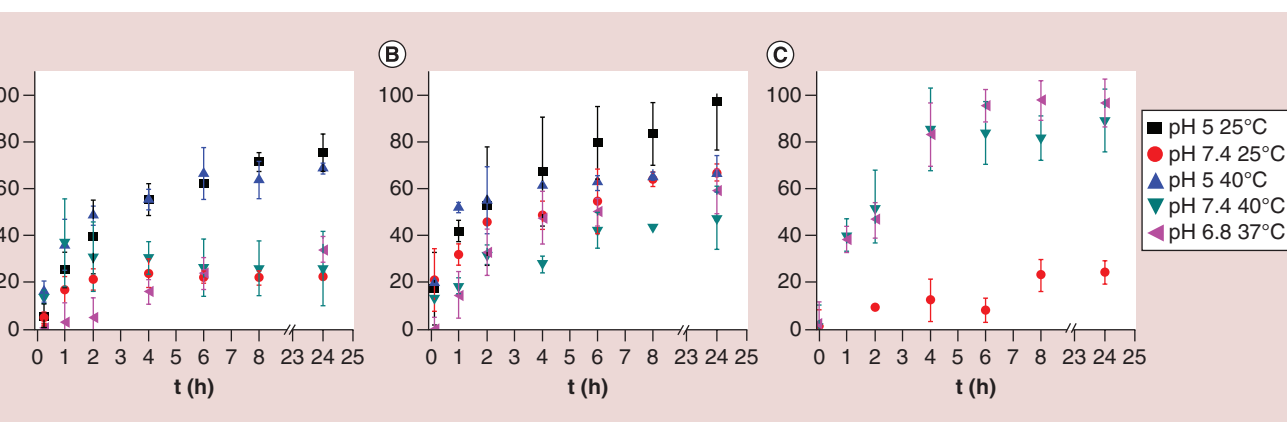
For their potential application in drug delivery, the encapsulation of an anticancer drug into the sIPN NGs (PNIPAM-s-AMPS 10% and PNIPAM-s-DMAEM 10%) was studied. The results of the encapsulation study are shown in Table 2.

With about 9% of loading capacity, PNIPAM-s-AMPS encapsulated twice the amount of DOXO compared with PNIPAM-s-DMAEM. For comparison, the loading capacity of PNIPAM/dPG NG without charges was between the loading capacities of both charged NGs. After the encapsulation, the release of DOXO was studied *in vitro*. For each NG, differ-

Table 2. Loading capacity (% L.C.) and loading efficiency (% L.E.) of doxorubicin; in poly-*N*-isopropylacrylamide/dPG, poly-*N*-isopropylacrylamide-*s*-2-acrylamido-2-methylpropane sulfonic acid and poly-*N*-isopropylacrylamide-*s*-(2-dimethylamino) ethyl methacrylate.

NG	%L.C.	%L.E.
PNIPAM/dPG	6.48	13.25
PNIPAM-s-AMPS	8.97	17.50
PNIPAM-s-DMAEM	4.30	9.00

AMPS: 2-acrylamido-2-methylpropane sulfonic acid; DMAEM: (2-dimethylamino) ethyl methacrylate; PNIPAM: Poly-*N*-isopropylacrylamide.



5. Cumulative release of DOXO from (A) PNIPAM-s-AMPS, (B) PNIPAM-s-DMAEM and (C) PNIPAM-dPG at different conditions and temperature.

2-acrylamido-2-methylpropane sulfonic acid; DOXO: Doxorubicin; DMAEM: (2-dimethylamino) ethyl methacrylate; M: Poly-*N*-isopropylacrylamide.

ent conditions were tested, below (25°C) and above (40°C) the T_p at pH 5 and 7.4 in order to analyze if the release had been triggered by temperature or pH and at pH 6.8 under body temperature which simulates the tumor microenvironment *in vivo* (Figure 5).

As expected, the release from PNIPAM-s-AMPS (Figure 5A) showed a pH dependent release with a faster and higher release of DOXO for both temperatures at pH 5. This behavior is due to the electrostatic interaction of the drug with the carrier at pH 7.4. At this neutral pH, the release was quite low and reached a value of 30% after 24 h, while at pH 5 a release of 70% is observed after 9 h. Moreover, this pH-dependent release is not so strong for PNIPAM-s-DMAEM (Figure 5B). For both the semi-interpenetrated NGs, under tumor microenvironment conditions the release was similar to the observed at pH 7.4 below and above the T_p , indicating that the trigger release is affected more by a strong change in pH than in temperature. When comparing with PNIPAM-dPG, the release is clearly driven by the collapse of the NG above the T_p since the network is not pH responsive. The performance of PNIPAM-s-AMPS/DOXO is highly desired for nanocarriers aiming to release the drug inside the lysosomes and not before their uptake into cells.

DOXO-resistant cancer cell proliferation inhibition *in vitro*

We compared the cancer cell proliferation inhibition performance of the DOXO-loaded NGs with free DOXO in two different cell lines: HeLa cells, which are sensitive to DOXO, and the HeLa-derived resistant cell line KB-V1 (Figure 6). Exposure of NGs and free DOXO to the cells was performed in the presence of serum and at the slightly elevated temperature of 40°C for 48 h in order to ensure seeing the effects above the

T_p of the NGs. The dose response curves of DOXO-loaded NGs, obtained by MTT Test, were similar to that of free DOXO in HeLa cells. The curve for PNIPAM-s-DMAEM showed a slightly different profile. For the DOXO resistant cell line (KB-V1) however, a concentration of free DOXO up to 10 μ M or DOXO encapsulated in PNIPAM-dPG up to 1 μ M caused no growth inhibition below \sim 90% relative viability. At this concentration, the DOXO-loaded NGs caused a reduction in cell viability to about 40%, while the dose-response curves appeared similar to the ones obtained with non-resistant cells.

Therapy of DOXO-resistant tumor *in vivo*

The tolerability and therapeutic effect of the SIPN NGs loaded with DOXO was studied *in vivo* in nude mice bearing a tumor from transplanted DOXO-resistant MaTu/ADR cells. Free DOXO and empty NGs mixed with free DOXO served as controls. First, we studied the tolerability of the nanocarriers and control compounds by monitoring body weight and blood composition for 39 days after intravenous administration. As it can be seen in Figure 7A, treatment with free DOXO in combination with empty NGs and with DOXO-loaded NGs caused a moderate and transient body weight reduction between -1.9 and -8.0%. DOXO-loaded NGs were slightly better tolerated than the corresponding combination of free DOXO and the empty NG. The formulations had no effect on red blood cells, platelets, hemoglobin, and hematocrit values (Supplementary Figure 2B–E, ESI). All formulations except of DOXO-loaded PNIPAM-s-DMAEM exhibited bone marrow toxicity as a side effect. All other formulations reduced the white blood cell number by up to 29% (Supplementary Figure 2A, ESI). A similar effect was observed for lymphocytes (Supplementary Figure 2F, ESI).

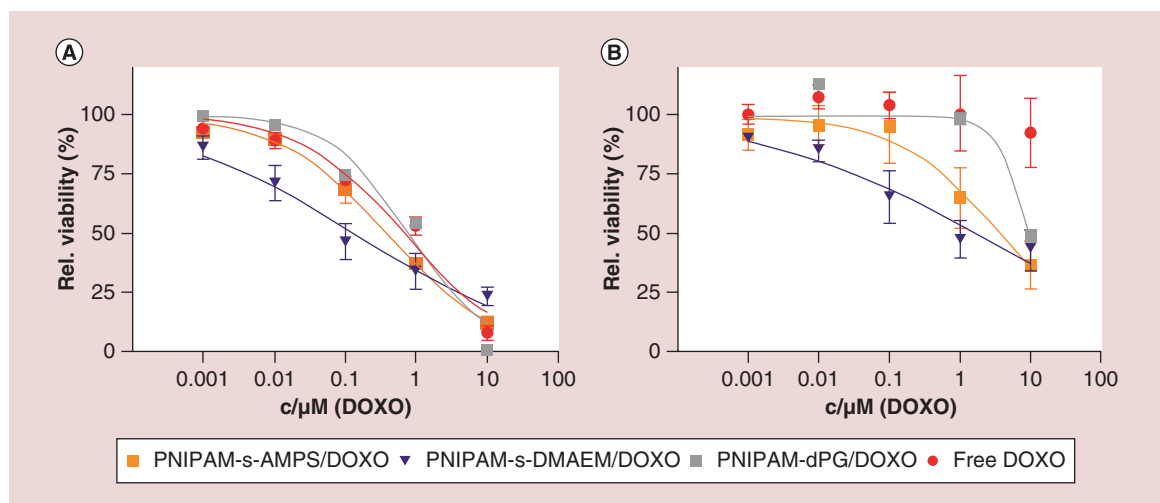


Figure 6. *In vitro* cancer cell proliferation inhibition of PNIPAM-s-AMPS/DOXO and PNIPAM-s-DMAEM/DOXO compared with PNIPAM-dPG/DOXO and free DOXO at 40°C (A) HeLa cells (B) (DOXO resistant) KB-V1 cells.

AMPS: 2-acrylamido-2-methylpropane sulfonic acid; DMAEM: (2-dimethylamino) ethyl methacrylate; DOXO: Doxorubicin; PNIPAM: Poly-*N*-isopropylacrylamide.

The strongest effect was observed after treatment with PNIPAM-dPG and PNIPAM-s-AMPS, both in combination with free DOXO, with a reduction of 35% (Supplementary Figure 2F, ESI). However, the mice recovered by the end of the study and the white blood cells and lymphocytes increased again to about the level of the control mice.

After the tolerability data was obtained, the therapeutic effect of the NGs was studied by monitoring the tumor volume (TV) during 39 days of treatment. Figure 7B summarizes the obtained results expressed as percentage tumor volume over control (T/C). In this study, free DOXO had a moderate inhibitory effect on the growth of the DOXO-resistant MaTu/ADR tumor with an inhibition of about 27% (T/C 73%). It can be clearly seen that only DOXO-loaded PNIPAM-s-AMPS caused a significant tumor growth inhibition of up to 75% (T/C 25%).

Discussion

The pH sensitive monomers DMAEM or AMPS were polymerized inside thermoresponsive PNIPAM-dPG NGs leading to sIPN NGs networks. Interestingly, the T_p values did not change after semi-interpenetration with the pH sensitive polymer. This is likely due to the fact that there was no covalent interaction between both interpenetrated materials, which left the thermosensitive properties almost unaffected, as already shown by a previous study by our group [36,37]. This invariability of the new system was advantageous compared with copolymerization, where the T_p shifted and widened [23,33]. As a general rule, the sizes of the NGs increased with the charge due to the osmotic

pressure. In the case of the sIPN NGs we observed a pH-dependent size change. For the positively charged PNIPAM-s-DMAEM, the size was decreased with increasing pH since the DMAEM is charged below pH 6.8, and for the negatively charged PNIPAM-s-AMPS, the size increased with increasing pH together with its charge density. This behavior was attributed to charge repulsion in the network that confers a more hydrophilic character to the NG, thus increasing its swelling ratio. More importantly, after the collapse of the NG, the ζ -potential of the network increased (Figure 3B & D) due to the exposure of the pH sensitive polymer on the surface of the NG following the collapse of the thermoresponsive network. This behavior can be exploited in different fields and applications, for example, to encapsulate or release a cargo on demand. On this regard, we have demonstrated the pH and thermo-release of proteins from sIPN NGs attached on honeycomb surfaces [37]. Several works have shown charge-conversional NGs [38–40] after a pH trigger but in the best of our knowledge this is the first time that the charge conversion is triggered by temperature.

The introduction of charged monomers into PNIPAM NGs is an extensively used strategy in order to increase the encapsulation of DOXO. For the negatively charged sIPN NGs, it was possible to double the encapsulation of DOXO. PNIPAM-s-AMPS encapsulated twice the amount of DOXO compared with PNIPAM-s-DMAEM, likely because of the electrostatic interaction. Even though we expect electrostatic repulsion, we observe about 4% loading capacity of DOXO inside the PNIPAM-s-DMAEM NGs; this is likely due to the partition of the drug in the NG/

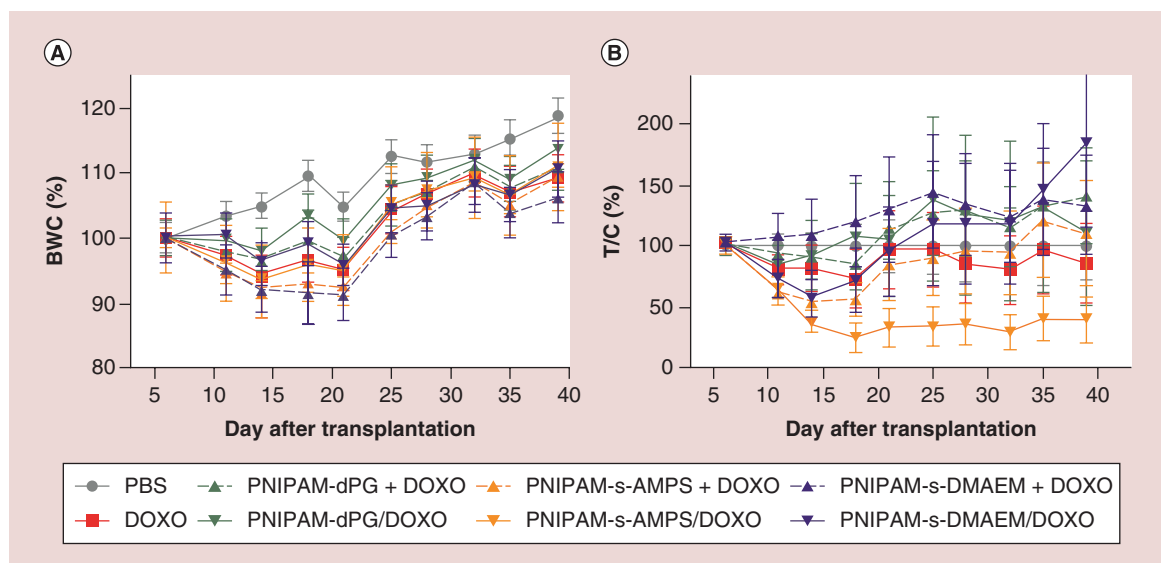


Figure 7. Treatment of nude mice bearing DOXO-resistant transplanted MaTu/ADR tumors. DOXO-loaded NGs (NG/DOXO) compared with free DOXO and empty NGs mixed with free DOXO (NG + DOXO) were applied at days 3 and 12. **(A)** Tolerability as monitored by body weight change over time (%) and **(B)** Therapeutic effect as monitored by change of tumor volume (percentage tumor over control T/C). DOXO: Doxorubicin.

water dispersion. The release profile of PNIPAM-s-AMPS showed an ideal behavior, with a slow release at pH 6.8 or 7.4 reaching a value of 30% after 24 h and a burst release at pH 5. The decreased diffusion of the drug at pH 6.8 and 7.4 could be assigned to the electrostatic attraction of the drug with the carrier. This result was very important to guarantee the low leakage of the drug until reaching the cytoplasm, thus overcoming resistance mechanisms in cancer cells, which confirms our hypothesis. The performance of the DOXO-loaded sIPN NG as drug carriers was studied by cancer cell proliferation inhibition of HeLa cells and HeLa-derived multidrug resistant KB-V1 cells. The contribution of nonspecific toxicity of the bare NG material was negligible at this range of concentrations tested, because 200 $\mu\text{g ml}^{-1}$ of NG which proved to be non toxic by MTT test (Figure 4) correlated to DOXO-loaded NG at 10 μM equivalents. At the slightly elevated temperature of 40°C we wanted to ensure to measure the effect of drug release from the NGs in the collapsed state. The comparison of the drug action at lower temperatures would not be meaningful in the cellular context since most physiological processes need 37°C for a regular function, and below 37°C drug action is impaired. Dose-response profiles of the NGs were overall similar to free DOXO, which indicated a different release in the cellular context than in the *in vitro* release studies. The difference here is that after cellular uptake, the NGs end up in perinuclear vesicles (Figure 4) which are probably acidic compartments such as lysosomes and we have shown that

the NGs can expose charged moieties upon a change of pH. DOXO would thereby be released near to the nucleus where it can intercalate in the DNA, rather than being transported out of the cell by P-gp which resides in the outer cell membrane. Multidrug-resistant cells (KB-V1) were resistant to free DOXO at the tested concentrations and to DOXO encapsulated in PNIPAM-dPG up to 1 μM , however DOXO encapsulated in the SIPN NGs could still efficiently inhibit cell proliferation, showing that SIPN NGs as drug carriers could indeed successfully bypass the resistance mechanism of the cells. Interestingly, on similar studies performed by our group using pH and thermo-sensitive NGs, no overcoming of the multidrug resistance was observed by DOXO-loaded NGs when the pH sensitive monomers are copolymerized [41].

Tolerability and therapeutic effect of nanocarriers are usually studied *in vivo* to check the feasibility of new materials to be applied in medicine. Through the evaluation of the tolerability of the NGs *in vivo*, we found similar effects on the body weight of all formulations and free DOXO. Similarly, blood composition analysis revealed no effects on red blood cells, platelets, hemoglobin and hematocrit. Nevertheless, a reduction in white blood cell counts was observed as known for free DOXO [42]. In this study, mice treated with PNIPAM-dPG only exhibited the same side effects, so we could conclude that the slightly enhanced toxicity of the NG/DOXO formulations on white blood cells compared with DOXO alone is a combination of both compounds. The reduction occurred at day 9

during treatment but the counts recovered until day 39. The therapeutic effect *in vivo* on DOXO-resistant tumor transplants was clearly seen only for PNIPAM-s-AMPS with encapsulated DOXO, as opposed to the mere combination of the two compounds. This difference observed for DOXO-loaded PNIPAM-s-AMPS is likely due to the slow release rate of DOXO, which could ensure that the drug was mainly being released after uptake into the cells and thereby could reach the nucleus or other sites of action rather than being expelled by the efflux transporter of the resistant cells that mediate the drug resistance. In our *in vitro* studies, both DOXO-loaded NGs were able to overcome drug resistance, which reflects the different cell exposure conditions in a cell culture dish compared with an organism. Here, a slower release mechanism seemed to be beneficial for both conditions.

Conclusion

Novel drug carriers were developed by semi-interpenetration of a pH sensitive polymer inside a thermoresponsive dendritic NG. These systems increased the superficial charge on demand, after an increase in temperature. The charge of the thermoresponsive NG could be fine-tuned by the choice of the pH sensitive polymer, the ratio of pH sensitive polymer per NG and the polymerization time of the pH sensitive polymer inside the NG. As a proof of concept, DOXO was encapsulated and efficiently released after a temperature trigger that was given by increasing the temperature. While encapsulation was increased due to the electrostatic interactions, the release was slower when this interaction was present. On the other hand, when electrostatic repulsion was observed, the release of the drugs was much faster.

Good cytocompatibility profile and internalization of NGs by tumor cells, important for a later use as drug carriers, were shown. In comparison with free DOXO, the loaded NGs were able to efficiently overcome the resistance mechanism of drug resistant tumor cells, resulting in an efficient proliferation inhibition. More importantly, DOXO-loaded PNIPAM-s-AMPS proved to efficiently overcome the resistance of tumor cells also *in vivo*. Hence, these pioneering SIPN NGs are promising drug carriers for cancer therapy.

Supplementary data

To view the supplementary data that accompany this paper please visit the journal website at: www.futuremedicine.com/doi/full/10.2217/nnm-2016-0308

Financial & competing interests disclosure

We gratefully acknowledge financial support from the Bundesministerium für Bildung und Forschung (BMBF) through the NanoMatFutur award (ThermoNanogele, 13N12561), the Helmholtz Virtual Institute "Multifunctional Biomaterials for Medicine", and the Freie Universität Berlin Focus Area Nanoscale. M Molina acknowledges financial support from the Alexander von Humboldt Foundation. The authors have no other relevant affiliations or financial involvement with any organization or entity with a financial interest in or financial conflict with the subject matter or materials discussed in the manuscript apart from those disclosed.

No writing assistance was utilized in the production of this manuscript.

Acknowledgements

We gratefully acknowledge P Winchester for proofreading the manuscript.

Executive summary

Background

- Semi-interpenetration of pH sensitive polymers inside thermoresponsive nanogels (NG) leads to potential drug carrier system with enhanced drug encapsulation and slower release to help overcome drug resistance mechanisms.

Methods

- Poly-*N*-isopropylacrylamide (PNIPAM)-dPG NGs were semi-interpenetrated with (2-dimethylamino) ethyl methacrylate (positively charged) or 2-acrylamido-2-methylpropane sulfonic acid (AMPS) (negatively charged) in different ratios and characterized regarding size and charges at different temperatures and pH.
- Doxorubicin (DOXO) encapsulation and release was studied *in vitro*.
- Cell proliferation inhibition of DOXO-loaded semi-interpenetrating polymer networks (SIPN) NG was studied on DOXO sensitive and resistant cells *in vitro* and in an *in vivo* tumor model.

Results

- PNIPAM NGs semi-interpenetrated with (2-dimethylamino) ethyl methacrylate or AMPS exposed charged moieties upon a thermal trigger.
- DOXO loading into SIPN NG was enhanced and release was slowed.
- Multidrug resistance could be overcome in cell culture by SIPN NG/DOXO.
- PNIPAM-s-AMPS/DOXO inhibited resistant tumor growth *in vivo* more efficiently than free DOXO.

Conclusion

- SIPN NG are a promising drug carrier for multidrug resistant cancer therapy.

References

- 1 WHO. *Cancer worldwide*. WHO Press, Geneva, Switzerland (2014).
- 2 Saenz Del Burgo L, Pedraz JL, Orive G. Advanced nanovehicles for cancer management. *Drug Discov. Today* 19(10), 1659–1670 (2014).
- 3 Chan A, Orme RP, Fricker RA, Roach P. Remote and local control of stimuli responsive materials for therapeutic applications. *Adv. Drug Deliv. Rev.* 65(4), 497–514 (2013).
- 4 Wang R, Billone PS, Mullett WM. Nanomedicine in action: an overview of cancer nanomedicine on the market and in clinical trials. *J. Nanomater.* 2013, 12 (2013).
- 5 Persidis A. Cancer multidrug resistance. *Nat. Biotechnol.* 17(1), 94–95 (1999).
- 6 Wu Q, Yang Z, Nie Y, Shi Y, Fan D. Multi-drug resistance in cancer chemotherapeutics: mechanisms and lab approaches. *Cancer Lett.* 347(2), 159–166 (2014).
- 7 Liang XJ, Chen C, Zhao Y, Wang PC. Circumventing tumor resistance to chemotherapy by nanotechnology. *Methods Mol. Biol.* 596, 467–488 (2010).
- 8 Yan Y, Björnalm M, Caruso F. Particle carriers for combating multidrug-resistant cancer. *ACS Nano* 7(11), 9512–9517 (2013).
- 9 Arora HC, Jensen MP, Yuan Y *et al.* Nanocarriers enhance Doxorubicin uptake in drug-resistant ovarian cancer cells. *Cancer Res.* 72(3), 769–778 (2012).
- 10 Ren W, Zeng L, Shen Z *et al.* Enhanced doxorubicin transport to multidrug resistant breast cancer cells via TiO₂ nanocarriers. *R. Soc. Chem. Adv.* 3(43), 20855–20861 (2013).
- 11 Oishi M, Hayashi H, Michihiro ID, Nagasaki Y. Endosomal release and intracellular delivery of anticancer drugs using pH-sensitive PEGylated nanogels. *J. Mater. Chem.* 17(35), 3720–3725 (2007).
- 12 Vijayaraghavalu S, Labhasetwar V. Efficacy of decitabine-loaded nanogels in overcoming cancer drug resistance is mediated via sustained DNA methyltransferase 1 (DNMT1) depletion. *Cancer Lett.* 331(1), 122–129 (2013).
- 13 Chacko RT, Ventura J, Zhuang J, Thayumanavan S. Polymer nanogels: a versatile nanoscopic drug delivery platform. *Adv. Drug Deliv. Rev.* 64(9), 836–851 (2012).
- 14 Kabanov AV, Vinogradov SV. Nanogels as pharmaceutical carriers: finite networks of infinite capabilities. *Angew Chem. Int. Ed. Engl.* 48(30), 5418–5429 (2009).
- 15 Bajpai AK, Shukla SK, Bhanu S, Kankane S. Responsive polymers in controlled drug delivery. *Prog. Poly. Sci.* 33(11), 1088–1118 (2008).
- 16 Qiu Y, Park K. Environment-sensitive hydrogels for drug delivery. *Adv. Drug Deliv. Rev.* 53(3), 321–339 (2001).
- 17 Cabane E, Zhang X, Langowska K, Palivan CG, Meier W. Stimuli-responsive polymers and their applications in nanomedicine. *Biointerphases* 7(1–4), 9–36 (2012).
- 18 Boutris C, Chatzi EG, Kiparissides C. Characterization of the LCST behaviour of aqueous poly(N-isopropylacrylamide) solutions by thermal and cloud point techniques. *Polymer* 38(10), 2567–2570 (1997).
- 19 Gao HF, Yang WL, Min K, Zha LS, Wang CC, Fu SK. Thermosensitive poly (N-isopropylacrylamide) nanocapsules with controlled permeability. *Polymer* 46(4), 1087–1093 (2005).
- 20 Giubudagian M, Asadian-Birjand M, Steinhilber D, Achazi K, Molina M, Calderon M. Fabrication of thermoresponsive nanogels by thermo-nanoprecipitation and *in situ* encapsulation of bioactives. *Poly. Chem.* 5(24), 6909–6913 (2014).
- 21 Asadian-Birjand M, Bergueiro J, Rancan F *et al.* Engineering thermoresponsive polyether-based nanogels for temperature dependent skin penetration. *Polym. Chem.* 6(32), 5827–5831 (2015).
- 22 Witting M, Molina M, Obst K *et al.* Thermosensitive dendritic polyglycerol-based nanogels for cutaneous delivery of biomacromolecules. *Nanomedicine* 11(5), 1179–1187 (2015).
- 23 Molina M, Giubudagian M, Calderón M. Positively charged thermoresponsive nanogels for anticancer drug delivery. *Macromol. Chem. Phys.* 215(24), 2414–2419 (2014).
- 24 Cuggino JC, Alvarez CI, Strumia MC *et al.* Thermosensitive nanogels based on dendritic polyglycerol and N-isopropylacrylamide for biomedical applications. *Soft. Matter* 7(23), 11259–11266 (2011).
- 25 Asadian-Birjand M, Bergueiro J, Wedepohl S, Calderón M. Near infrared dye conjugated nanogels for combined photodynamic and photothermal therapies. *Macromol. Biosci.* 16(10), 1432–1441 (2016).
- 26 Rancan F, Asadian-Birjand M, Dogan S *et al.* Effects of thermoresponsivity and softness on skin penetration and cellular uptake of polyglycerol-based nanogels. *J. Control. Release* 228, 159–169 (2016).
- 27 Kim S, Healy KE. Synthesis and characterization of injectable poly(N-isopropylacrylamide-co-acrylic acid) hydrogels with proteolytically degradable cross-links. *Biomacromolecules* 4(5), 1214–1223 (2003).
- 28 Lopez-Leon T, Ortega-Vinuesa JL, Bastos-Gonzalez D, Elaissari A. Cationic and anionic poly(N-isopropylacrylamide) based submicron gel particles: electrokinetic properties and colloidal stability. *J. Phys. Chem. B.* 110(10), 4629–4636 (2006).
- 29 Kawano T, Niidome Y, Mori T, Katayama Y, Niidome T. PNIPAM gel-coated gold nanorods for targeted delivery responding to a near-infrared laser. *Bioconj. Chem.* 20(2), 209–212 (2009).
- 30 Kumar CS, Mohammad F. Magnetic nanomaterials for hyperthermia-based therapy and controlled drug delivery. *Adv. Drug Deliv. Rev.* 63(9), 789–808 (2011).
- 31 Molina MA, Rivarola CR, Miras MC, Lescano D, Barbero CA. Nanocomposite synthesis by absorption of nanoparticles into macroporous hydrogels. Building a chemomechanical actuator driven by electromagnetic radiation. *Nanotechnology* 22(24), 245504 (2011).
- 32 Thimma Reddy T, Takahara A. Simultaneous and sequential micro-porous semi-interpenetrating polymer network hydrogel films for drug delivery and wound dressing applications. *Polymer* 50(15), 3537–3546 (2009).

- 33 Molina MA, Rivarola CR, Barbero CA. Effect of copolymerization and semi-interpenetration with conducting polyanilines on the physicochemical properties of poly(N-isopropylacrylamide) based thermosensitive hydrogels. *Eur. Polym. J.* 47(10), 1977–1984 (2011).
- 34 Haag R, Tuerk H, Mecking S: DE10211664 A1 (2003).
- 35 Stein U, Walther W, Stege A, Kaszubiak A, Fichtner I, Lage H. Complete *in vivo* reversal of the multidrug resistance phenotype by jet-injection of anti-MDR1 short hairpin RNA-encoding plasmid DNA. *Mol. Ther.* 16(1), 178–186 (2008).
- 36 Molina M, Wedepohl S, Calderon M. Polymeric near-infrared absorbing dendritic nanogels for efficient *in vivo* photothermal cancer therapy. *Nanoscale* 8(11), 5852–5856 (2016).
- 37 De León AS, Molina M, Wedepohl S, Muñoz-Bonilla A, Rodríguez-Hernández J, Calderón M. Immobilization of stimuli-responsive nanogels onto honeycomb porous surfaces and controlled release of proteins. *Langmuir* 32(7), 1854–1862 (2016).
- 38 Chen W, Achazi K, Schade B, Haag R. Charge-conversional and reduction-sensitive poly(vinyl alcohol) nanogels for enhanced cell uptake and efficient intracellular doxorubicin release. *J. Control. Release* 205, 15–24 (2015).
- 39 Zhang X, Zhang K, Haag R. Multi-stage, charge conversional, stimuli-responsive nanogels for therapeutic protein delivery. *Biomater. Sci.* 3(11), 1487–1496 (2015).
- 40 Du J-Z, Sun T-M, Song W-J, Wu J, Wang J. A tumor-acidity-activated charge-conversional nanogel as an intelligent vehicle for promoted tumoral-cell uptake and drug delivery. *Angew. Chem. Int. Ed.* 49(21), 3621–3626 (2010).
- 41 Cuggino JC, Molina M, Wedepohl S, Igarzabal CIA, Calderón M, Gugliotta LM. Responsive nanogels for application as smart carriers in endocytic pH-triggered drug delivery systems. *Eur. Polym. J.* 78 14–24 (2016).
- 42 Bonadonna G, Monfardini S, De Lena M, Fossati-Bellani F, Beretta G. Phase I and preliminary phase II evaluation of adriamycin (NSC 123127). *Cancer Res.* 30(10), 2572–2582 (1970).